Bismuth Sillenite Crystals as Recent Photocatalysts for Water Treatment and Energy Generation: A Critical Review

O. Baaloudj, H. Kenfoud, A.K. Badawi, A. El Jery, A.A. Assadi, A. Amrane

catalysts

MDPI

Review

Bismuth Sillenite Crystals as Recent Photocatalysts for Water Treatment and Energy Generation: A Critical Review

Oussama Baaloudj [1,*], Hamza Kenfoud [1], Ahmad K. Badawi [2], Achraf Amir Assadi [3], Atef El Jery [4], Aymen Amine Assadi [5] and Abdeltif Amrane [5,*]

1 Laboratory of Reaction Engineering, Faculty of Mechanical Engineering and Process Engineering, USTHB, BP 32, Algiers 16111, Algeria; hamza.kenfoud.93@gmail.com
2 Civil Engineering Department, El-Madina Higher Institute for Engineering and Technology, Giza 12588, Egypt; dr.ahmedkaram91@gmail.com
3 Research Unit Advanced Materials, Applied Mechanics, Innovative Processes and Environment, Higher Institute of Applied Sciences and Technology of Gabes (ISSAT), University of Gabes, Sfax 3018, Tunisia; achraf.assadi@gmail.com
4 Department of Chemical Engineering, College of Engineering, King Khalid University, Abha 61411, Saudi Arabia; ajery@kku.edu.sa
5 Ecole Nationale Supérieure de Chimie de Rennes, University of Rennes, ISCR-UMR 6226, F-35000 Rennes, France; aymen.assadi@ensc-rennes.fr
* Correspondence: obaaloudj@usthb.dz (O.B.); abdeltif.amrane@univ-rennes1.fr (A.A.)

Abstract: Photocatalysis has been widely studied for environmental applications and water treatment as one of the advanced oxidation processes (AOPs). Among semiconductors that have been employed as catalysts in photocatalytic applications, bismuth sillenite crystals have gained a great deal of interest in recent years due to their exceptional characteristics, and to date, several sillenite material systems have been developed and their applications in photoactivity are under study. In this review paper, recent studies on the use of Bi-based sillenites for water treatment have been compiled and discussed. This review also describes the properties of Bi-based sillenite crystals and their advantages in the photocatalytic process. Various strategies used to improve photocatalytic performance are also reviewed and discussed, focusing on the specific advantages and challenges presented by sillenite-based photocatalysts. Furthermore, a critical point of certain bismuth catalysts in the literature that were found to be different from that reported and correspond to the sillenite form has also been reviewed. The effectiveness of some sillenites for environmental applications has been compared, and it has demonstrated that the activity of sillenites varies depending on the metal from which they were produced. Based on the reviewed literature, this review summarizes the current status of work with binary sillenite and provides useful insights for its future development, and it can be suggested that Bismuth sillenite crystals can be promising photocatalysts for water treatment, especially for degrading and reducing organic and inorganic contaminants. Our final review focus will emphasize the prospects and challenges of using those photocatalysts for environmental remediation and renewable energy applications.

Keywords: bismuth; sillenite; semiconductor; photocatalysis; water treatment

Citation: Baaloudj, O.; Kenfoud, H.; Badawi, A.K.; Assadi, A.A.; El Jery, A.; Assadi, A.A.; Amrane, A. Bismuth Sillenite Crystals as Recent Photocatalysts for Water Treatment and Energy Generation: A Critical Review. *Catalysts* **2022**, *12*, 500. https://doi.org/10.3390/catal12050500

Academic Editors: Qian Zhang and Yu Huang

Received: 9 April 2022
Accepted: 26 April 2022
Published: 29 April 2022

1. Introduction

Water is the most important natural resource on our planet; its resources are one of the essential aspects of every society's sustainable development [1,2]. The water quality is critical in addition to its quantity [3]. Even though water covers more than 71% of the Earth's surface, approximately only 2.5% of it is fresh water and only 0.002% is considered available to humans [4]. Although this quantity is limited, it is constantly contaminated by harmful chemicals generated by human activities such as agricultural discharge, poor sanitation, and rapid industrialization [5,6]. These contaminants are challenging to eliminate, and their presence in water has negative impacts on both health and environmental

factors [7]. As a result of the fast advancement of science and technology, industries have risen and evolved, and the developing chemical industry has synthesized a large number of chemical compounds so far [8,9]. More and more hazardous compounds are being created and released into the water environment and their concentrations are continuously increasing [10].

Several pieces of research have provided a critical overview of the various treatment strategies for treating contaminated water [1]. Contaminated water cannot be adequately treated using conventional methods. Conventional physical and biological techniques, such as adsorption, reverse osmosis, and air stripping, can only extract soluble organic materials [11–13]. In actuality, they do not completely eliminate pollutants, they rather transfer them from one phase to another [14]. In general, these techniques have considerable drawbacks and disadvantages, one of which is contamination with treatment by-products, which can increase the risk of cancer and pollute the environment [15,16]. Therefore, developing innovative methods and approaches for treating water and wastewater is very necessary [6]. In contrast to conventional approaches, advanced oxidation processes (AOPs) have exhibited satisfactory performances in the past few decades. They have shown to be a better solution for the rapid removal of non-biodegradable compounds in water [17,18]. AOPs use hydroxyl radicals and other powerful oxidizing agents to efficiently remove dangerous contaminants via direct or indirect mechanisms [19,20]. These radicals may react with a wide range of contaminants and produce hydroxylated or dehydrogenated products, which can then be mineralized into non-toxic final products such as water (H_2O) and carbon dioxide (CO_2), as well as inorganic ions [21]. Pollutant mineralization is the strong point of these processes because it completely removes environmental pollutants [22].

As one of the AOP techniques, photocatalysis is one of the best approaches, as it very efficiently opens new avenues for addressing global energy needs and pollution issues [23,24]. It has aroused the interest of the scientific community in recent decades, particularly as one of the most effective applications for the removal of organic and inorganic pollutants [25]. It is also known that photocatalysis is capable of producing chemical reactions that are highly thermodynamically demanding that would otherwise require energy-intensive inputs in terms of an elevated temperature (or pressure), which are potentially beneficial in energy generation and environmental cleaning applications [26]. Issues directly related to human health and environmental health such as the purity of water and air can be effectively addressed through photocatalysis as it will be one of the most important future technologies for all kinds of photocatalysts in the field of environmental treatment [27]. Heterogeneous photocatalysis using semiconductors as catalysts is more efficient in environmental applications because they are very efficient, easy to produce, and use a heterogeneous process that makes it easy to separate them from water [24,28]. Semiconductors also have other properties suitable for photocatalytic reactions, such as their optical absorption characteristics, their electronic structure, and the capacity to form charge carriers when energized with a light source by transforming light energy into chemical energy [17,21]. Highly effective and eco-friendly metal oxide semiconductor types have been developed. For example, TiO_2 (Yao et al. 2003b) is widely considered the most photoactive of all catalysts. However, TiO_2's disadvantages, such as its high photo-generated electron–hole pair recombination rate and poor irradiation sensitivity due to its large energy band gap, limit its practical applicability [29]. To overcome these obstacles, it is necessary to develop innovative, efficient, and multifunctional semiconductors with excellent photocatalytic activities, an appropriate photo-generated pair recombination rate, and a low band gap [30–32].

The core metal ion for photocatalysts is considered to be one of the most critical aspects in the development of new semiconductors [33], with titanium (Ti), bismuth (Bi), zinc (Zn), and tin (Sn) being the best metals for semiconductor synthesis [34]. Bismuth semiconductors have become incredibly valuable recently due to their superior chemical stability, strong light absorption, low pair recombination rate, and low optical band gap [34,35]. "Bi" ions are indeed harmful and hazardous when they are free, especially in the form of nitrate.

However, their risks can be reduced by using them to synthesize chemically stable semiconductors without an ionic state. This contributes to waste management by lowering harmful ions and synthesizing valuable materials that can be used for environmental purposes. For this purpose, this review takes on bismuth semiconductors as an exciting topic.

2. Bismuth Sillenite Crystals

As is well known, semiconductors based on the transition-metal ion of Bi^{3+} have become attractive because of the proprieties of those ions [24], such as:

(i) Their d10 configuration in the oxide lattices makes photo-generated electron–hole pairs easier to separate [36].
(ii) Their $6s^2$ orbital lone pair does not have any bonding or sharing with other atoms, which can potentially produce a structural disruption by inducing repulsive effects on neighbors' bonding. It can also create an internal polar electric field in crystallites, increasing the probability of charge separation due to the opposing movements of electron–hole pairs in the electric field [33,37].
(iii) Their ability to narrow the band gap by the orbital hybridization between O 2p and Bi 6s in the semiconductor's valence band allows photo-induced holes to move in the valence band [33,36].

Those phenomena can aid the photocatalytic activities in Bismuth-based semiconductors. Within the bismuth semiconductors category, the most exciting class is that of sillenite crystals. These crystals have attracted a great deal of scientific attention because of their unique structure of crystals [33], high photorefractive [38,39] and photochromic properties [40], dielectric properties [41], electro-optic properties [42], fast response [41,43], long optical storage time in the dark [44], recyclability, and narrow band gap (<2.9 eV) [36,45]. Recently, sillenite-type materials have been widely applied in a number of applications such as optical data processing and storage, electro-optics, acoustics, peizotechnics, optoelectronic, electronics, fiber optic sensor, image amplification, real-time and multiwavelength hologram imaging, metrological problems, and a variety of photocatalysis applications [46–50]. Bismuth oxide crystals with the sillenite structure, as defined by the general formula $Bi_{12}[M]O_{20}$ (BMO), where M is the tetravalent ion of the elements from II–VIII groups of the Periodic Table, are a body-centered cubic crystal structure with the space group I23 [51–53]. Figure 1 shows the crystal structure of the perfect $Bi_{12}MO_{20}$ sillenite and local structure around the Bi and the M sites. The general structure of the BMO structure is described by a bismuth atom (Bi^{3°) surrounded by eight oxygen atoms that share corners with other comparable polyhedra BiO_8 and tetravalent ions MO_4 that occur both at the cube center and on the corners of the cube [54–60].

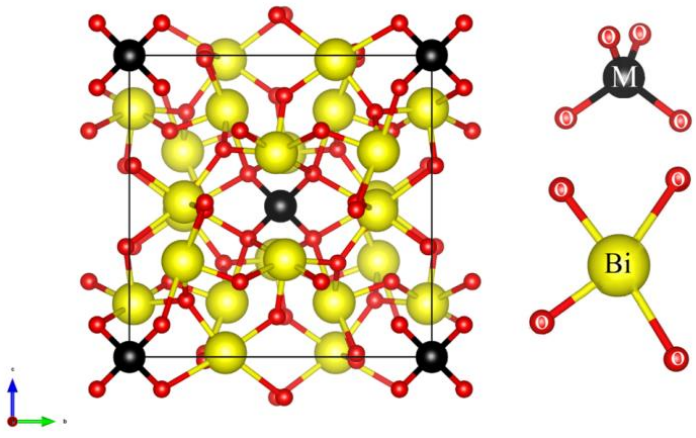

Figure 1. Crystal structure of the perfect $Bi_{12}MO_{20}$ and local structure around the Bi and the M sites [61].

There is a critical point of certain bismuth catalysts in the literature that was different from those reported and corresponds to the sillenite stoichiometric model. In fact, bismuth catalysts generally form a sillenite phase when calcined in an air oven, where the probability of obtaining another phrase similar to spinel is very low. However, several studies considered their catalyst to be another phase, such as spinel, where they were sillenites, but it was difficult to determine the phase in their samples due to low information in the X-ray diffraction database about sillenites. For example, there is a great number of works (Kumar et al., 2018 [62]; Thi Mai Tho et al., 2018 [63]; Dang et al., 2019 [64]; Habibi-yangjeh et al., 2020 [65]; Nguyen et al., 2020 [66]; Nithya and Ayyappan, 2020 [67]; Baaloudj et al., 2021a [68]; Bahadoran et al., 2021b [69]) that reports the synthesis of $ZnBi_2O_4$; however, their phases were more compatible with sillenite phase $Bi_{12}ZnO_{20}$ (PDF #78-1325 [70]) and far from the spinel phase $ZnBi_2O_4$ (JCPDS: 43-0449 [71]). Another example, the synthesis of $CoBi_2O_4$, was reported in two works [7,72], although the phases were more consistent with the sillenite phase $Bi_{12}CoO_{20}$ [34,73].

There has recently been a surge in research on sillenite-phase semiconductors for various photocatalytic applications. Series of sillenite semiconductors $Bi_{12}CoO_{20}$ [34], $Bi_{12}TiO_{20}$ [25], $Bi_{12}NiO_{19}$ [58], and $Bi_{12}ZnO_{20}$ [32,70] were studied, and they showed high photoactivity against various kinds of pollutants. So, it was exciting to scan the literature and summarize recent works that dealt with sillenite crystals as photocatalysts for water treatment and environmental application.

3. Sillenites as Recent Photocatalysts

Semiconductor nanostructures have the potential to revolutionize the disciplines of photocatalytic oxidation and heterogeneous catalysis through the combined effects of quantum confinement and unique surface conformations [27]. The sillenite-type crystals $Bi_{12}MO_{20}$ have been the subject of extensive research to understand and adapt the material's properties for a variety of applications [48]. Extensive study of the photocatalytic applications of sillenite-structured crystals began in the mid-2000s, with many new sillenites being used as photocatalysts in previous research [51]. Various types of pollutants have been used in the application of sillenites. Among them, there are organic pollutants such as dyes and antibiotics, and there are also inorganic pollutants such as hexavalent chromium; however, the most frequently used contaminant for sillenites application in the literature was the antibiotic cefixime. Table 1 lists bibliographical references using sillenite crystals for water photocatalytic treatment for various pollutants. Not only were sillenites with the formula $Bi_{12}MO_{20}$ undertaken in this summary, but even Bi-based sillenites with other stoichiometric qualities were also taken. The majority of the research mentioned in the table was recent.

Table 1. Sillenite photocatalysts for environmental applications.

Sillenite	Synthesis Route	Target Pollutants	Operating Conditions	Removal Efficiency	Ref.
$Bi_{12}TiO_{20}$	Sol-gel	Cefixime	Dose of catalyst: 1.5 g/L pH: 6 Time of irradiation: 4 h Pollutant concentration: 10 mg/L	94.93%	[25]
$Bi_{12}ZnO_{20}$	Sol-gel	Cefixime	Dose of catalyst: 1 g/L pH: 6 Time of irradiation: 4 h Pollutant concentration: 10 mg/L	94.34%	[70]
$Bi_{12}ZnO_{20}$	Sol-gel	Hexavalent chromium	Dose of catalyst: 1 g/L pH: 6 Time of irradiation: 3 h Pollutant concentration: 30 mg/L	77.19%	[70]

Table 1. *Cont.*

Sillenite	Synthesis Route	Target Pollutants	Operating Conditions	Removal Efficiency	Ref.
$Bi_{12}ZnO_{20}$	Co-precipitation	Cefuroxime	Dose of catalyst: 1 g/L pH: 6 Time of irradiation: 4 h Pollutant concentration: 15 mg/L	80%	[32]
$Bi_{12}CoO_{20}$	Sol-gel	Basic Red 46	Dose of catalyst: 1 g/L pH: 6 Time of irradiation: 3 h Pollutant concentration: 15 mg/L	86%	[34]
$Bi_{12}CoO_{20}$	Sol-gel	Hexavalent chromium	Dose of catalyst: 1 g/L pH: 6 Time of irradiation: 3 h Pollutant concentration: 15 mg/L	67%	[34]
$Bi_{12}NiO_{19}$	Sol-gel	Basic blue 41	Dose of catalyst: 1 g/L pH: 9 Time of irradiation: 180 min Pollutant concentration: 15 mg/L	98%	[58]
$Bi_{12}SiO_{20}$	Pechini sol-gel	Rhodamine B	Reaction time: 150 min Pollutant concentration: 10 mg/L	80%	[23]
$Bi_{12}TiO_{20}$	Oxidant peroxide	Rhodamine B	Dose of catalyst: 60 mg pH: 6 Time of irradiation: 210 min Pollutant concentration: 10 mg/L	81%	[74]
$Bi_{12}TiO_{20}$	Simple solution phase	Methyl orange	Dose of catalyst: 1.6 g/L Time of irradiation: 150 min Pollutant concentration: 150 mg/L	75%	[75]
$Bi_{12}GeO_{20}$	Chemical solution decomposition	Methyl orange	Dose of catalyst: 6 g/L Time of irradiation: 50 min Pollutant concentration: 25 mg/L	100%	[29]
$Bi_{12}MnO_{20}$	Sol-gel	Hexavalent chromium	Dose of catalyst: 2 g/L pH: 6, Time of irradiation: 4 h Pollutant concentration: 10 mg/L	80%	[36]
$Bi_{12}FeO_{20}$	Hydrothermal	Methylene blue and Congo red	Time of irradiation: 3.5 h Pollutant concentration: 3.5 mg/L and 10 mg/L	91.8% and 32.10%	[60]
$Bi_{25}VO_{40}$	Facile pechini	Methylene blue	Dose of catalyst: 0.16 g/L Time of irradiation: 240 min Pollutant concentration: 10 mg/L	90%	[33]
$Bi_{24}AlO_{39}$	Chemical solution decomposition	Methyl Orange	Dose of catalyst: 6 g/L pH: 2, Time of irradiation: 2 h Pollutant concentration: 20 mg/L	100%	[37]
$Bi_{25}GaO_{39}$	Solid state reaction	Methylen blue	Dose of catalyst: 2 g/L, Time of irradiation: 60 min Pollutant concentration: 10 mg/L	89%	[49]
$Bi_{12}SiO_{20}$ $Bi_{12}GeO_{20}$ $Bi_{12}TiO_{20}$	Solid state reaction	Rhodamine B	Dose of catalyst: 3 g/L, pH: 6, Time of irradiation: 6 h Pollutant concentration: 20 mg/L	80%, 30% and 90%	[28]
$Bi_{12}GeO_{20}$ $Bi_{12}SiO_{20}$ $Bi_{12}TiO_{20}$	Facile electrospining	Rhodamine B	Dose of catalyst: 80 mg pH: 6, Time of irradiation: 120 min Pollutant concentration: 10 mg/L	100%, 80% and 100%	[24]
$Bi_{12}PbO_{19}$ $Bi_{12}NiO_{19}$ $Bi_{24}AlO_{39}$ $Bi_{12}TiO_{20}$ $Bi_{36}Fe_2O_{57}$	Chemical solution decomposition	Methyl Orange	Dose of catalyst: 0.25 g pH: 6, Aqueous methyl orange solution: 50 mL	100% With different $t_{1/2}$	[76]

As can be seen from the table, the reported sillenites have proven to be effective at removing various pollutants; however, the application has only focused on organic pollutants such as antibiotics and dyes and inorganic contaminants such as heavy pollutants metals. This creates the need to test those photocatalysts for other uses, such as disinfecting water from bacteria and viruses, as photocatalysis has already proven to be an effective process for this [1,2]. Another note from the table is that all reported sillenites showed almost complete efficiency, but unfortunately in different conditions, so it would be interesting to compare some of these catalysts under the same conditions for the same pollutant.

4. Sillenites Catalysts for Hydrogen Generation

The depletion of non-renewable energies and the increase in environmental pollution in our time raises many concerns and insists on the development of renewable and clean energy technologies. Currently, researchers are putting high levels of effort into reducing dependence on non-renewable energy resources and trying to find effective alternatives to green energy. In this regard, H_2 has been recognized as a clean fuel due to its zero-emissions combustion nature, and could become the most widely used fuel in the future [77]. The production of hydrogen gas (H_2) is one of the most important alternatives and the cleanest energy carrier for these purposes. Hydrogen generation via photocatalytic water separation (PWS) is an important strategy to facilitate global clean energy and overcome the severe environmental challenges facing our society today [78]. Photocatalysis using active catalysts is a method that makes it possible to obtain an energy source from renewable sources, in other words, water and the sun, without producing waste. One of the unique advantages of the photocatalyst lies in the possibility of using it in water purification and hydrogen generation at the same time [79] it can also be used with solar energy to become an ecological and inexpensive process that is very easy to use on an industrial scale. In the context of the current status, there are several photocatalytic materials reported so far for H_2 evolution reaction. Generally, the examination of the performance of these photocatalysts is based on two factors, (i) the quantity of the H_2 evolved and (ii) the reusability and recyclability of the catalysts. Sillenites can be relied on (Figure 2) as has already been demonstrated in a previous work showing that sillenites such as $Bi_{12}CoO_{20}$ can be used in the hydrogen generation process as an alternative to green energy due to its favorable and excellent optical and electrochemical properties [34]. Another experimental study of catalytic hydrogen production also supports the prediction made by the previous study where the sillenite $Bi_{25}FeO_{40}$ showed significantly better performance and much higher hydrogen production compared to other types of nanoparticles [80]. Although little work has been performed on the use of sillenite in the hydrogen generation process, its ease of synthesis and its excellent physical and photoelectric properties predict its effectiveness to become one of the most important photocatalysts in this field. Therefore, different sillenite compounds should be used as photocatalysts and tested in different techniques to improve the photocatalytic efficiency and thus increase hydrogen production or reduce the time required for wastewater treatment, especially to make full use of solar radiation and obtain higher photocatalytic activity. This will be one of the most important goals and work must be performed to find and improve the excellent and effective mechanisms using sillenite crystals that can benefit humanity in the future.

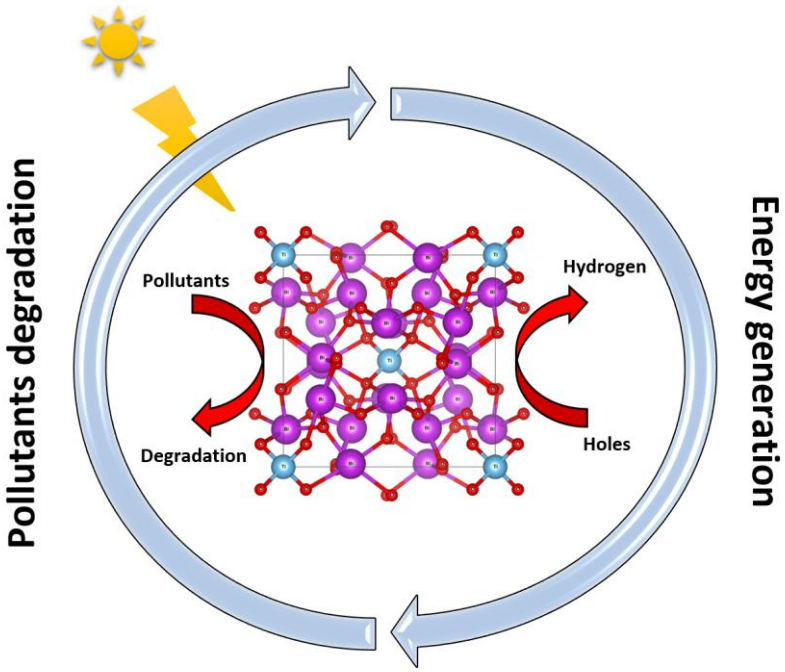

Figure 2. Sillenites for environmental applications: Pollutants degradation and energy generation.

5. Comparative Study of Some Sillenite Catalysts

Based on our recent research that dealt with the characterization and application of the sillenites $Bi_{12}TiO_{20}$ (BTO), $Bi_{12}CoO_{20}$ (BCO), $Bi_{12}ZnO_{20}$ (BZO), and $Bi_{12}NiO_{19}$ (BNO) for environmental applications, it is now feasible to compare their efficiency in terms of pollution removal. All those sillenites were synthesized by the sol-gel method, and the detailed method for each material can be found in the following works [25,34,58,70]. Cefixime (CFX) was chosen as the target pollutant since it was used in most of those works. A comparative test was conducted using the sillenites BTO, BCO, BZO, and BNO in order to remove CFX antibiotics from water. The photocatalytic tests were carried out in a double-walled stirred reactor (batch). The photocatalytic conditions were chosen based on past research [25,70], with a concentration C_{CFX} = 10 mg/L, pH ~ 6, T = 25 °C, and dose of catalyst = 1 g/L. Before exposing those tests to irradiation sources (UV light), all sets were combined in the dark for 120 min to avoid the adsorption effect and establish the adsorption–desorption equilibrium. Figure 3 demonstrated the CFX degradation tests using those sillenites under the same conditions. As observed, CFX degradation using BZO and BTO as catalysts achieved almost relative efficiency of 94.34% and 88.07%, respectively, within 180 min, while this was lower for the others. The sillenite BCO has also shown a good degradation performance, giving 71.23% within 180 min. However, the sillenite BNO has shown a very low degradation efficiency for CFX, although it has given a very efficient degradation for Basic blue 41. The low efficiency of the sillenite BNO may be explained by the fact that BNO photodegradation can be enhanced in the basic condition [58]; however, CFX photodegradation is favored in the neutral medium of approximately 6 [25]; therefore, the two are incompatible. This phenomenon may be due to the surface charge of both the catalyst and the pollutant. The differences in the efficiency of each sillenite may be due to the color and gap energy of the catalysts, which provides a higher level of light absorption for both BTO and BZO in the range of 200–600 nm, which is very close to the UV region. The degree of crystallinity and the purity of the phase also play a major role in determining the efficiency of the catalyst. In the end, BZO proved to be the most efficient catalyst for the removal of CFX, with a degradation rate of 94.34% in just 3 h.

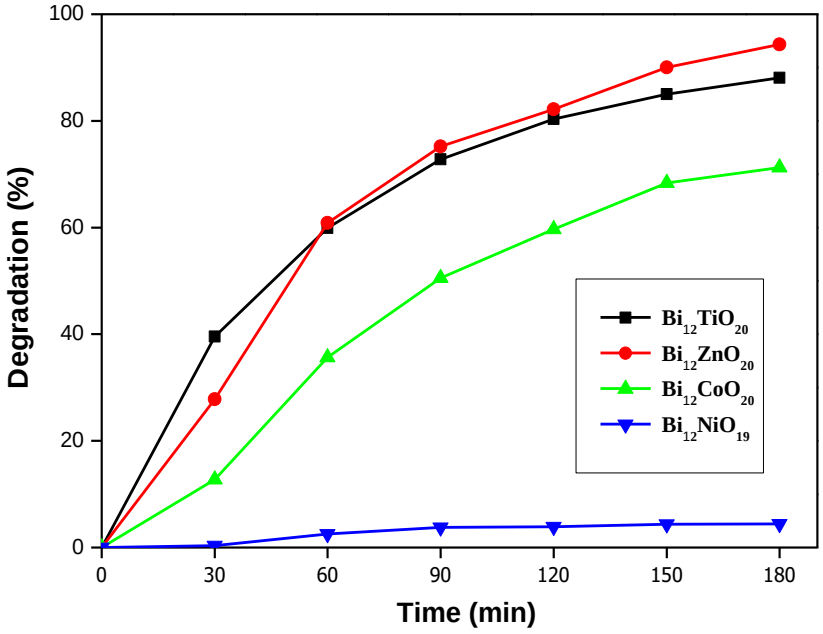

Figure 3. CFX degradation using different sillenite photocatalysts. C_{CFX} = 10 mg/L, pH ~ 6, T = 25 °C and dose of catalyst = 1 g/L.

6. Combining of Sillenite with Other Processes

Several strategies can be utilized to improve the photocatalytic activity of these interesting sillenites, such as ion doping, the presence of other reactive species, the addition of H_2O_2, hybrid systems, and morphology modification (Figure 4). However, only a few studies of sillenites as photocatalysts coupled with other strong oxidants have been published, leaving a gap in our knowledge of these important materials. This section will address some of the available references in this field.

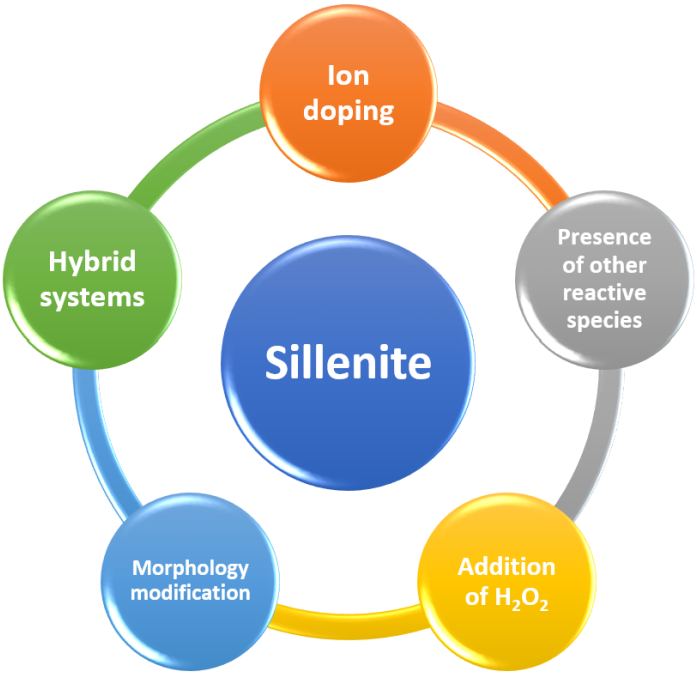

Figure 4. Various strategies used to improve the photocatalytic performance of sillenites.

According to the work of Liu et al. 2018 [81], a hydrothermal technique was used to create the sillenite bismuth ferrite (S-BFO) $Bi_{25}FeO_{40}$, which was then used to activate peroxymonosulfate (PMS) in the degradation of aquatic levofloxacin. It was confirmed that a decay mechanism could proceed as follows: (i) Bi^{5+} is replaced by Bi^{3+}, resulting in the formation of an oxygen vacancy in the lattice and active oxygen (O^*), which could produce reactive species such as $SO_4{}^*$ through reactions with PMS. This study demonstrates that the photocatalytic activity of the $Bi_{25}FeO_{40}$ catalyst in the presence of PMS as a source of the reactive species could be adopted alternatively in the decontamination of surface/groundwater.

Moreover, from the work of Naghmash et al., 2021 [82], it was shown that the addition of hydrogen peroxide (H_2O_2) with the sillenite $Bi_{12}SiO_{20}$ (BS) and the doped sillenite M-$Bi_{12}SiO_{20}$ with transition metal ions (M = Mn, Cu, Co, Ni or Fe) as catalysts allow for chemical decomposition to form reactive species such as OH^*. The performance of the $Bi_{12}SiO_{20}$ catalyst was markedly improved with the addition of H_2O_2.

It was also proven that the doping of $Bi_{12}MO_{20}$ (M = Ge, Si, Ti) crystals with elements in different valence states has a significant effect on their optical, photoelectric, and acoustic properties [83]. Another study on $Bi_{12}ZnO_{20}$ demonstrated that doping the sillenites with an ion such as Ag can increase the electronic life (photosensitization), which means a higher recombination rate of the photogenerated electron–hole pairs [70].

7. Summary and Outlooks

This review discusses the effects of advances in nanoscience and photocatalysis for present and future applications, focusing on bismuth sillenite crystals that have attracted much attention as photocatalysts in water photocatalytic treatment in recent years due to their excellent properties. Recent studies on the use of Bi-based sillenites for water treatment have been compiled and discussed; they exhibited efficient photocatalytic performances for a large type of pollutants, including organic pollutants such as antibiotics and inorganic contaminants such as heavy metals. The features of bismuth-based semiconductors have been reported, as well as their advantages in the photocatalytic process. Bismuth-based semiconductors have features due to the properties of Bi^{3+} ions, which include (i) the d10 configuration in the lattices of the oxide, (ii) the $6s^2$ orbital lone pair, and (iii) the orbital hybridization between O 2p and Bi 6s in the valence band of the semiconductor. The advantages that the Bi^{3+} ions provide in terms of photocatalytic activity are (i) the decrease in the recombination of photo-generated charges, which facilities the interfacial charge transfer, (ii) the production of an internal polar electric field in crystallites, which increases the probability of charge separation due to the opposing movements of electron–hole pairs in the electric field, and (iii) the narrowing of the band gap. The advantages of the sillenite structure were also discussed. They are (i) the unique structures of the crystal, (ii) high photorefractive ability, (iii) fast response, (iv) photochromic, dielectric, and electro-optic properties, (v) long optical storage time in the dark, (vi) recyclability, and (vii) the narrow band gap, which is less than 2.9 eV. A critical point concerning certain bismuth catalysts in the literature has also been reviewed; they reported bismuth spinel, which was found to be different from that reported and conformed to the form of sillenite. Finally, the effectiveness of certain sillenites for environmental applications has been compared, and it has been demonstrated that the activity of sillenites varies depending on the metal from which they were produced. $Bi_{12}ZnO_{20}$ proved to be the most efficient catalyst because the Zn ions enhanced the photocatalytic activity. Although there are reports on the photocatalytic activity of these materials, detailed studies on these compounds are limited. More efforts are needed to understand the properties and relationships of such bismuth sillenites-based compounds and their optimization of photocatalytic activity. Understanding the link between this research, especially concerning photocatalytic activity, will aid in the development of more effective photocatalysts. Up to now, there has been a great number of works that have dealt with bismuth sillenites as photocatalysts in photocatalysis applications; however, those works focused not only on organic pollutants such as antibiotics and dyes and inorganic

contaminants such as heavy metals but also on the possibility of using sillenite in the process of hydrogen generation to become an effective alternative resource for green energy. More efforts are required for the practical application in other uses, such as disinfecting water from bacteria and viruses. Based on this updated literature, bismuth sillenite crystals appear to be promising photocatalysts for water treatment, particularly for degrading and reducing organic and inorganic contaminants.

Author Contributions: O.B. and A.A.A. (Achraf Amir Assadi), writing—original draft preparation; A.K.B. and H.K., writing—review and editing; A.E.J., A.A.A. (Aymen Amine Assadi) and A.A., supervision and editing. All authors have read and agreed to the published version of the manuscript.

Funding: This research received no external funding.

Data Availability Statement: Not applicable.

Acknowledgments: This work was supported by the King Khalid University, Abha, Saudi Arabia (by grant R.G.P. 1/195/42). We express our gratitude to the Deanship of Scientific Research, King Khalid University, for its support of this study. The authors thank the USTHB, ENSCR, Higher Institute for Engineering and Technology and ISSATG for their scientific collaboration.

Conflicts of Interest: The authors declare no conflict of interest.

References

1. Baaloudj, O.; Assadi, I.; Nasrallah, N.; El, A.; Khezami, L. Simultaneous removal of antibiotics and inactivation of antibiotic-resistant bacteria by photocatalysis: A review. *J. Water Process Eng.* **2021**, *42*, 102089. [CrossRef]
2. Elgohary, E.A.; Mohamed, Y.M.A.; El Nazer, H.A.; Baaloudj, O.; Alyami, M.S.S.; El Jery, A.; Assadi, A.A.; Amrane, A. A Review of the Use of Semiconductors as Catalysts in the Photocatalytic Inactivation of Microorganisms. *Catalysts* **2021**, *11*, 1498. [CrossRef]
3. Gökkuş, Ö.; Yıldız, Y.Ş. Application of electro-Fenton process for medical waste sterilization plant wastewater. *Desalin. Water Treat.* **2016**, *57*, 24934–24945. [CrossRef]
4. Kaczala, F.; Blum, S.E. The Occurrence of Veterinary Pharmaceuticals in the Environment: A Review. *Curr. Anal. Chem.* **2015**, *12*, 169–182. [CrossRef] [PubMed]
5. Khan, S.T.; Malik, A. Engineered nanomaterials for water decontamination and purification: From lab to products. *J. Hazard. Mater.* **2019**, *363*, 295–308. [CrossRef]
6. Benrighi, Y.; Nasrallah, N.; Chaabane, T.; Sivasankar, V.; Darchen, A.; Baaloudj, O. Photocatalytic performances of $ZnCr_2O_4$ nanoparticles for cephalosporins removal: Structural, optical and electrochemical properties. *Opt. Mater.* **2021**, *115*, 111035. [CrossRef]
7. Baaloudj, O.; Nasrallah, N.; Kebir, M.; Guedioura, B.; Amrane, A.; Nguyen-Tri, P.; Nanda, S.; Assadi, A.A. Artificial neural network modeling of cefixime photodegradation by synthesized $CoBi_2O_4$ nanoparticles. *Environ. Sci. Pollut. Res.* **2020**, *28*, 15436–15452. [CrossRef]
8. Boyd, C.E. Water Quality Protection. In *Water Quality: An Introduction*; Springer International Publishing: Cham, Switzerland, 2020; pp. 379–409, ISBN 978-3-030-23335-8.
9. Lou, W.; Kane, A.; Wolbert, D.; Rtimi, S.; Assadi, A.A. Study of a photocatalytic process for removal of antibiotics from wastewater in a falling film photoreactor: Scavenger study and process intensification feasibility. *Chem. Eng. Process. Process Intensif.* **2017**, *122*, 213–221. [CrossRef]
10. Patnaik, P. *Handbook of Environmental Analysis: Chemical Pollutants in Air, Water, Soil, and Solid Wastes*, 3rd ed.; CRC Press: Boca Raton, FL, USA, 2017. [CrossRef]
11. Li, B.; Zhang, T. Biodegradation and adsorption of antibiotics in the activated sludge process. *Environ. Sci. Technol.* **2010**, *44*, 3468–3473. [CrossRef]
12. Gao, Y.; Li, Y.; Zhang, L.; Huang, H.; Hu, J.; Shah, S.M.; Su, X. Adsorption and removal of tetracycline antibiotics from aqueous solution by graphene oxide. *J. Colloid Interface Sci.* **2012**, *368*, 540–546. [CrossRef]
13. Chen, W.R.; Huang, C.H. Adsorption and transformation of tetracycline antibiotics with aluminum oxide. *Chemosphere* **2010**, *79*, 779–785. [CrossRef]
14. Achour, S.; Amokrane, S.; Chegrouche, S.; Nibou, D.; Baaloudj, O. Artificial neural network modeling of the hexavalent uranium sorption onto chemically activated bentonite. *Res. Chem. Intermed.* **2021**, *47*, 4837–4854. [CrossRef]
15. Brahimi, B.; Mekatel, E.; Mellal, M.; Baaloudj, O.; Brahimi, R.; Hemmi, A.; Trari, M.; Belmedani, M. Enhanced photodegradation of acid orange 61 by the novel hetero-junction $CoFe_2O_4$/AgCl. *Opt. Mater.* **2021**, *121*, 111576. [CrossRef]
16. Benrighi, Y.; Nasrallah, N.; Chaabane, T.; Sivasankar, V.; Darchen, A.; Baaloudj, O. Characterization of $CoCr_2O_4$ semiconductor: A prominent photocatalyst in the degradation of basic blue 41 from wastewater. *Opt. Mater.* **2021**, *122*, 111819. [CrossRef]
17. Kenfoud, H.; Nasrallah, N.; Baaloudj, O.; Meziani, D.; Chaabane, T.; Trari, M. Photocatalytic reduction of Cr(VI) onto the spinel $CaFe_2O_4$ nanoparticles. *Optik* **2020**, *223*, 165610. [CrossRef]

18. Kenfoud, H.; Nasrallah, N.; Baaloudj, O.; Derridj, F.; Trari, M. Enhanced photocatalytic reduction of Cr(VI) by the novel hetero-system $BaFe_2O_4/SnO_2$. *J. Phys. Chem. Solids* **2022**, *160*, 110315. [CrossRef]
19. Bourkeb, K.; Baaloudj, O. Facile electrodeposition of ZnO on graphitic substrate for photocatalytic application: Degradation of antibiotic in a continuous stirred-tank reactor. *J. Solid State Electrochem.* **2021**, *26*, 573–580. [CrossRef]
20. Asadi-Ghalhari, M.; Mostafaloo, R.; Ghafouri, N.; Kishipour, A.; Usei, S.; Baaloudj, O. Removal of Cefixime from aqueous solutions via proxy electrocoagulation: Modeling and optimization by response surface methodology. *React. Kinet. Mech. Catal.* **2021**, *134*, 459–471. [CrossRef]
21. Akerdi, A.G.; Bahrami, S.H. Application of heterogeneous nano-semiconductors for photocatalytic advanced oxidation of organic compounds: A review. *J. Environ. Chem. Eng.* **2019**, *7*, 103283. [CrossRef]
22. Baaloudj, O.; Nasrallah, N.; Kebir, M.; Khezami, L.; Amrane, A.; Assadi, A.A. A comparative study of ceramic nanoparticles synthesized for antibiotic removal: Catalysis characterization and photocatalytic performance modeling. *Environ. Sci. Pollut. Res.* **2020**, *28*, 13900–13912. [CrossRef]
23. Wu, Y.; Chang, X.; Li, M.; Hei, X.P.; Liu, C.; Zhang, X. Studying the preparation of pure $Bi_{12}SiO_{20}$ by Pechini method with high photocatalytic performance. *J. Sol.-Gel Sci. Technol.* **2021**, *97*, 311–319. [CrossRef]
24. Hou, D.; Hu, X.; Wen, Y.; Shan, B.; Hu, P.; Xiong, X.; Qiao, Y.; Huang, Y. Electrospun sillenite $Bi_{12}MO_{20}$ (M = Ti, Ge, Si) nanofibers: General synthesis, band structure, and photocatalytic activity. *Phys. Chem. Chem. Phys.* **2013**, *15*, 20698–20705. [CrossRef]
25. Baaloudj, O.; Nasrallah, N.; Bouallouche, R.; Kenfoud, H.; Khezami, L.; Assadi, A.A. High efficient Cefixime removal from water by the sillenite $Bi_{12}TiO_{20}$: Photocatalytic mechanism and degradation pathway. *J. Clean. Prod.* **2022**, *330*, 129934. [CrossRef]
26. Kanhere, P.; Chen, Z. A review on visible light active perovskite-based photocatalysts. *Molecules* **2014**, *19*, 19995–20022. [CrossRef]
27. Abrams, B.L.; Wilcoxon, J.P. Nanosize Semiconductors for Photooxidation. *Crit. Rev. Solid State Mat. Sci.* **2005**, *30*, 153–182. [CrossRef]
28. Noh, T.H.; Hwang, S.W.; Kim, J.U.; Yu, H.K.; Seo, H.; Ahn, B.; Kim, D.W.; Cho, I.S. Optical properties and visible light-induced photocatalytic activity of bismuth sillenites ($Bi_{12}XO_{20}$, X = Si, Ge, Ti). *Ceram. Int.* **2017**, *43*, 12102–12108. [CrossRef]
29. He, C.; Gu, M. Photocatalytic activity of bismuth germanate $Bi_{12}GeO_{20}$ powders. *Scr. Mater.* **2006**, *54*, 1221–1225. [CrossRef]
30. Muthukrishnaraj, A.; Arun, A.; Kalaivani, S.S.; Maiyalagan, T.; Manikandan, A.; Balasubramanian, N. Solvothermal synthesis and characterizations of graphene-$ZnBi_{12}O_{20}$ nanocomposites for visible-light driven photocatalytic applications. *Ceram. Int.* **2020**, *46*, 18534–18543. [CrossRef]
31. Yao, W.F.; Wang, H.; Xu, X.H.; Zhang, Y.; Yang, X.N.; Shang, S.X.; Liu, Y.H.; Zhou, J.T.; Wang, M. Characterization and photocatalytic properties of Ba doped $Bi_{12}XO_{20}$. *J. Mol. Catal. A Chem.* **2003**, *202*, 305–311. [CrossRef]
32. Baaloudj, O.; Nasrallah, N.; Assadi, A.A. Facile synthesis, structural and optical characterizations of $Bi_{12}ZnO_{20}$ sillenite crystals: Application for Cefuroxime removal from wastewater. *Mater. Lett.* **2021**, *304*, 130658. [CrossRef]
33. Qiao, X.; Pu, Y.; Li, Y.; Huang, Y.; Cheng, H.; Seo, H.J. Structural characteristics and photocatalytic ability of vanadate-sillenite $Bi_{25}VO_{40}$ nanoparticles. *Powder Technol.* **2016**, *287*, 277–284. [CrossRef]
34. Kenfoud, H.; Baaloudj, O.; Nasrallah, N.; Bagtache, R.; Assadi, A.A.; Trari, M. Structural and electrochemical characterizations of $Bi_{12}CoO_{20}$ sillenite crystals: Degradation and reduction of organic and inorganic pollutants. *J. Mater. Sci. Mater. Electron.* **2021**, *32*, 16411–16420. [CrossRef]
35. Tho, N.T.M.; Khanh, D.N.N.; Thang, N.Q.; Lee, Y.I.; Phuong, N.T.K. Novel reduced graphene oxide/$ZnBi_2O_4$ hybrid photocatalyst for visible light degradation of 2,4-dichlorophenoxyacetic acid. *Environ. Sci. Pollut. Res.* **2020**, *27*, 11127–11137. [CrossRef] [PubMed]
36. Wu, X.; Li, M.; Li, J.; Zhang, G.; Yin, S. A sillenite-type $Bi_{12}MnO_{20}$ photocatalyst: UV, visible and infrared lights responsive photocatalytic properties induced by the hybridization of Mn 3d and O 2p orbitals. *Appl. Catal. B Environ.* **2017**, *219*, 132–141. [CrossRef]
37. Yao, W.F.; Xu, X.H.; Zhou, J.T.; Yang, X.N.; Zhang, Y.; Shang, S.X.; Wang, H.; Huang, B.B. Photocatalytic property of sillenite $Bi_{24}AlO_{39}$ crystals. *J. Mol. Catal. A Chem.* **2004**, *212*, 323–328. [CrossRef]
38. Valant, M.; Suvorov, D. A stoichiometric model for sillenites. *Chem. Mater.* **2002**, *14*, 3471–3476. [CrossRef]
39. Oliveira, T.M.; Santos, C.; Lima, A.F.; Lalic, M.V. Antisite defect as rule for photorefractive, photochromic and photocatalytic properties of $Bi_{12}MO_{20}$ (M = Ge, Si, Ti) sillenite crystals. *J. Alloys Compd.* **2017**, *720*, 187–195. [CrossRef]
40. Nogueira, A.E.; Longo, E.; Leite, E.R.; Camargo, E.R. Visible-light photocatalysis with bismuth titanate ($Bi_{12}TiO_{20}$) particles synthesized by the oxidant peroxide method (OPM). *Ceram. Int.* **2015**, *41*, 12073–12080. [CrossRef]
41. Delice, S.; Isik, M.; Gasanly, N.M.; Darvishov, N.H.; Bagiev, V.E. Structural and temperature-tuned optical characteristics of $Bi_{12}GeO_{20}$ sillenite crystals. *Chinese J. Phys.* **2020**, *66*, 422–429. [CrossRef]
42. Wu, Y.; Lu, J.; Li, M.; Yuan, J.; Wu, P.; Chang, X.; Liu, C.; Wang, X. Bismuth silicate photocatalysts with enhanced light harvesting efficiency by photonic crystal. *J. Alloys Compd.* **2019**, *810*, 151839. [CrossRef]
43. Zhang, X.; Zhang, L.; Hu, J.S.; Pan, C.L.; Hou, C.M. Facile hydrothermal synthesis of novel $Bi_{12}TiO_{20}$-Bi_2WO_6 heterostructure photocatalyst with enhanced photocatalytic activity. *Appl. Surf. Sci.* **2015**, *346*, 33–40. [CrossRef]
44. Zhang, H.; Lü, M.; Liu, S.; Xiu, Z.; Zhou, G.; Zhou, Y.; Qiu, Z.; Zhang, A.; Ma, Q. Preparation and photocatalytic properties of sillenite $Bi_{12}TiO_{20}$ films. *Surf. Coatings Technol.* **2008**, *202*, 4930–4934. [CrossRef]
45. Isik, M.; Sarigul, N.; Gasanly, N.M. Thermoluminescence characteristics of $Bi_{12}SiO_{20}$ single crystals. *J. Lumin.* **2020**, *224*, 117280. [CrossRef]
46. Marrakchi, A.; Johnson, R.V.; Tanguay, A.R. Polarization properties of enhanced self-diffraction in sillenite crystals. *IEEE J. Quantum Electron.* **1987**, *23*, 2142–2151. [CrossRef]
47. Reyher, H.J.; Hellwig, U.; Thiemann, O. Optically detected magnetic resonance of the bismuth-on-metal-site intrinsic defect in photorefractive sillenite crystals. *Phys. Rev. B* **1993**, *47*, 5638–5645. [CrossRef]

48. Ahmad, I.; Marinova, V.; Goovaerts, E. High-frequency electron paramagnetic resonance of the hole-trapped antisite bismuth center in photorefractive bismuth sillenite crystals. *Phys. Rev. B—Condens. Matter Mater. Phys.* **2009**, *79*, 2–5. [CrossRef]
49. Lin, X.; Huang, F.; Wang, W.; Xia, Y.; Wang, Y.; Liu, M.; Shi, J. Photocatalytic activity of a sillenite-type material $Bi_{25}GaO_{39}$. *Catal. Commun.* **2008**, *9*, 572–576. [CrossRef]
50. Deng, C.; Wei, X.; Liu, R.; Du, Y.; Pan, L.; Zhong, X.; Song, J. Synthesis of sillenite-type $Bi_{36}Fe_2O_{57}$ and elemental bismuth with visible-light photocatalytic activity for water treatment. *Front. Mater. Sci.* **2018**, *12*, 415–425. [CrossRef]
51. Burkov, V.I.; Egorysheva, A.V.; Kargin, Y.F. Optical and chiro-optical properties of crystals with sillenite structure. *Crystallogr. Reports* **2001**, *46*, 312–335. [CrossRef]
52. Kim, B.H.; Lim, T.H.; Roh, J.W.; Lee, S.G.; Ju, C.S.; Park, S.S.; Hong, S.S.; Lee, G.D. Effect of Cr doping on the properties and photocatalytic activity of $Bi_{12}TiO_{20}$. *React. Kinet. Mech. Catal.* **2010**, *99*, 217–224. [CrossRef]
53. Meng, X.; Zhang, G.; Li, N. $Bi_{24}Ga_2O_{39}$ for visible light photocatalytic reduction of Cr(VI): Controlled synthesis, facet-dependent activity and DFT study. *Chem. Eng. J.* **2017**, *314*, 249–256. [CrossRef]
54. Valant, M.; Suvorov, D. Processing and Dielectric Properties of Sillenite Compounds $Bi_{12}MO_{20}$-δ (M: Si, Ge, Ti, Pb, Mn, $B_{1/2}P_{1/2}$). *ChemInform* **2010**, *33*, 2900–2904. [CrossRef]
55. Zhoua, P.; Xiaoa, F.; Jia, L. $Bi_{12}NiO_{19}$ micro-sheets grown on graphene oxide: Temperature-dependent facile synthesis and excellent electrochemical behavior for supercapacitor electrode. *J. Electroanal. Chem.* **2021**, *884*, 115075. [CrossRef]
56. Pei, L.Z.; Wei, T.; Lin, N.; Zhang, H. Synthesis of bismuth nickelate nanorods and electrochemical detection of tartaric acid using nanorods modified electrode. *J. Alloys Compd.* **2016**, *663*, 677–685. [CrossRef]
57. Rajamoorthy, M.; Geetha, D.; Sathiya Priya, A. Synthesis of Cobalt-Doped $Bi_{12}NiO_{19}$: Structural, Morphological, Dielectric and Magnetic Properties. *Arab. J. Sci. Eng.* **2021**, *46*, 737–744. [CrossRef]
58. Brahimi, B.; Kenfoud, H.; Benrighi, Y.; Baaloudj, O. Structural and Optical Properties of $Bi_{12}NiO_{19}$ Sillenite Crystals: Application for the Removal of Basic Blue 41 from Wastewater. *Photochem* **2021**, *1*, 319–329. [CrossRef]
59. Deng, H.; Hao, W.; Xu, H. First-principles calculations of novel sillenite compounds $Bi_{24}M_2O_{40}$ (M = Se or Te). *Rare Met.* **2011**, *30*, 135–139. [CrossRef]
60. Vavilapalli, D.S.; Melvin, A.A.; Bellarmine, F.; Mannam, R.; Velaga, S.; Poswal, H.K.; Dixit, A.; Ramachandra Rao, M.S.; Singh, S. Growth of sillenite $Bi_{12}FeO_{20}$ single crystals: Structural, thermal, optical, photocatalytic features and first principle calculations. *Sci. Rep.* **2020**, *10*, 22052. [CrossRef]
61. Lima, A.F.; Lalic, M. V First-principles study of the $BiMO_4$ antisite defect in the $Bi_{12}MO_{20}$ (M = Si, Ge, Ti) sillenite compounds. *J. Phys. Condens. Matter* **2013**, *25*, 495505. [CrossRef]
62. Kumar, K.V.; Shilpa, C.H.; Rama, C.K.; Rajesham, K.A. Synthesis & Structural Characteristics of $ZnBi_2O_4$ Nanoparticles Prepared by Citrate-Gel Auto Combustion Method. *Int. J. Nanoparticle Res.* **2018**, *2*, 1–7. [CrossRef]
63. Thi Mai Tho, N.; The Huy, B.; Nha Khanh, D.N.; Quoc Thang, N.; Thi Phuong Dieu, N.; Dai Duong, B.; Thi Kim Phuong, N. Mechanism of Visible-Light Photocatalytic Mineralization of Indigo Carmine Using $ZnBi_2O_4$-Bi2S3 Composites. *ChemistrySelect* **2018**, *3*, 9986–9994. [CrossRef]
64. Dang, K.; Thang, N.Q.; Thi, N. Visible-light driven $Bi_2S_3/ZnBi_2O_4$ hybrid catalysts for efficient photocatalytic degradation of Rhodamine B. *VIETNAM J. CHEM* **2019**, *4*, 358–365.
65. Habibi-yangjeh, A.; Pirhashemi, M.; Ghosh, S. $ZnO/ZnBi_2O_4$ nanocomposites with p-n heterojunction as durable visible-light-activated photocatalysts for efficient removal of organic pollutants. *J. Alloys Compd.* **2020**, *826*, 154229. [CrossRef]
66. Nguyen, V.H.; Mousavi, M.; Ghasemi, J.B.; van Le, Q.; Delbari, S.A.; Namini, A.S.; Asl, M.S.; Shokouhimehr, M.; Mohammadi, M. Novel p−n heterojunction nanocomposite: TiO_2 Qds/$ZnBi_2O_4$ photocatalyst with considerably enhanced photocatalytic activity under visible-light irradiation. *J. Phys. Chem. C* **2020**, *124*, 27519–27528. [CrossRef]
67. Nithya, R.; Ayyappan, S. Novel exfoliated graphitic-C3N4 hybridised $ZnBi_2O_4$ (g-C3N4/$ZnBi_2O_4$) nanorods for catalytic reduction of 4-Nitrophenol and its antibacterial activity. *J. Photochem. Photobiol. A Chem.* **2020**, *398*, 112591. [CrossRef]
68. Baaloudj, O.; Assadi, A.A.; Azizi, M.; Kenfoud, H.; Trari, M.; Amrane, A.; Assadi, A.A.; Nasrallah, N. Synthesis and Characterization of $ZnBi_2O_4$ Nanoparticles: Photocatalytic Performance for Antibiotic Removal under Different Light Sources. *Appl. Sci.* **2021**, *11*, 3975. [CrossRef]
69. Bahadoran, A.; Masudy-Panah, S.; De Lile, J.R.; Li, J.; Gu, J.J.; Sadeghi, B.; Ramakrishna, S.; Liu, Q. Novel 0D/1D $ZnBi_2O_4$/ZnO S-scheme photocatalyst for hydrogen production and BPA removal. *Int. J. Hydrogen Energy* **2021**, *46*, 24094–24106. [CrossRef]
70. Baaloudj, O.; Nasrallah, N.; Kenfoud, H.; Algethami, F.; Modwi, A.; Guesmi, A.; Assadi, A.A.; Khezami, L. Application of $Bi_{12}ZnO_{20}$ Sillenite as an Efficient Photocatalyst for Wastewater Treatment: Removal of Both Organic and Inorganic Compounds. *Materials* **2021**, *14*, 5409. [CrossRef]
71. Bahadoran, A.; Farhadian, M.; Hoseinzadeh, G.; Liu, Q. Novel flake-like Z-Scheme Bi_2WO_6-$ZnBi_2O_4$ heterostructure prepared by sonochemical assisted hydrothermal procedures with enhanced visible-light photocatalytic activity. *J. Alloys Compd.* **2021**, *883*, 160895. [CrossRef]
72. Jagadeesh, C.; Sailaja, B.B. V Photocatalytic Degradation of Rohdamine B Dye using $CoBi_2O_4$ Nanocatalyst and Effect of Various Operational Parameters. *Cikitusi J.* **2019**, *6*, 97–107.
73. Elkhouni, T.; Amami, M.; Ben Salah, A. Structural, spectroscopic studies and magnetic properties of doped sillenites-type oxide Bi_{12}[M]O_{20} M=Fe, Co. *J. Supercond. Nov. Magn.* **2013**, *26*, 2997–3004. [CrossRef]
74. Nogueira, A.E.; Lima, A.R.F.; Longo, E.; Leite, E.R.; Camargo, E.R. Structure and photocatalytic properties of Nb-doped $Bi_{12}TiO_{20}$ prepared by the oxidant peroxide method (OPM). *J. Nanoparticle Res.* **2014**, *16*, 2653. [CrossRef]

75. Hou, J.; Qu, Y.; Krsmanovic, D.; Ducati, C.; Eder, D.; Kumar, R.V. Solution-phase synthesis of single-crystalline $Bi_{12}TiO_{20}$ nanowires with photocatalytic properties. *Chem. Commun.* **2009**, *26*, 3937–3939. [CrossRef]
76. Yao, W.F.; Wang, H.; Xu, X.H.; Zhou, J.T.; Yang, X.N.; Zhang, Y.; Shang, S.X.; Wang, M. Sillenites materials as novel photocatalysts for methyl orange decomposition. *Chem. Phys. Lett.* **2003**, *377*, 501–506. [CrossRef]
77. Kumar, A.; Krishnan, V. Vacancy Engineering in Semiconductor Photocatalysts: Implications in Hydrogen Evolution and Nitrogen Fixation Applications. *Adv. Funct. Mater.* **2021**, *31*, 2009807. [CrossRef]
78. Cao, S.; Piao, L.; Chen, X. Emerging Photocatalysts for Hydrogen Evolution. *Trends Chem.* **2020**, *2*, 57–70. [CrossRef]
79. Kenfoud, H.; Nasrallah, N.; Baaloudj, O.; Belabed, C.; Chaabane, T.; Trari, M. Opto-electrochemical characteristics of synthesized $BaFe_2O_4$ nanocomposites: Photocatalytic degradation and hydrogen generation investigation. *Int. J. Hydrogen Energy* **2022**, *47*, 12039–12051. [CrossRef]
80. Basith, M.A.; Ahsan, R.; Zarin, I.; Jalil, M.A. Enhanced photocatalytic dye degradation and hydrogen production ability of $Bi_{25}FeO_{40}$-rGO nanocomposite and mechanism insight. *Sci. Rep.* **2018**, *8*, 33–35. [CrossRef] [PubMed]
81. Liu, Y.; Guo, H.; Zhang, Y.; Tang, W.; Cheng, X.; Li, W. Heterogeneous activation of peroxymonosulfate by sillenite $Bi_{25}FeO_{40}$: Singlet oxygen generation and degradation for aquatic levofloxacin. *Chem. Eng. J.* **2018**, *343*, 128–137. [CrossRef]
82. Naghmash, M.A.; Saif, M.; Mahmoud, H.R. Transition metal ions doped $Bi_{12}SiO_{20}$ as novel catalysts for the decomposition of hydrogen peroxide (H_2O_2). *J. Taiwan Inst. Chem. Eng.* **2021**, *121*, 268–275. [CrossRef]
83. Chmyrev, V.I.; Skorikov, V.M.; Larina, E.V. Doping effect on the optical, electro-optic, and photoconductive properties of $Bi_{12}MO_{20}$ (M = Ge, Si, Ti). *Inorg. Mater.* **2006**, *42*, 381–392. [CrossRef]